J. Mater. Environ. Sci. 5 (2) (2014) 615-624
ISSN : 2028-2508
CODEN: JMESCN

Non-isothermal kinetic and thermodynamic studies of the dehydroxylation process of synthetic calcium hydroxide $Ca(OH)_2$

M. Khachani*, A. El Hamidi, M. Halim, S. Arsalane
Laboratoire de Physico-Chimie des Matériaux, Catalyse et Environnement, Université Mohammed V- Agdal, Faculté des Sciences, Avenue Ibn Batouta, BP:1014, 10000 Rabat Principal, Morocco

Received 9 Oct 2013, Revised 10 Dec 2013, Accepted 10 Dec 2013
**Corresponding author. E-mail: mariamkhachani@gmail.com; Tel: (+212 537 77 54 40)*

Abstract
The non-isothermal kinetics of dehydroxylation of $Ca(OH)_2$ have been studied in dynamic helium atmosphere using TG, DTG, DTA and XRD techniques at different heating rates. The apparent activation energy E_α is determined using Friedman and advanced isoconversional methods (Model-Free). The results indicate that dehydroxylation process occurs predominantly by an irreversible major step, preceded by a rapid and reversible one. The Malek's kinetic procedure associated with non-linear regression approach was used to determine the pre-exponential factor (A) and the kinetic model function. The autocatalytic SB (Systak-Berggren) reaction model corresponding to differential function $f(\alpha) = \alpha^m.(1-\alpha)^n$ is the most probable for the dehydroxylation process of $Ca(OH)_2$. The best fit has led to following kinetic triplet: $Ln\ A$ = 16.85, E = 132.20 kJ.mol^{-1} and $f(\alpha) = \alpha^{0.203}.(1-\alpha)^{0.380}$. The thermodynamic functions (ΔS^*, ΔH^*, ΔG^*) of the studied reaction are calculated using activated complex theory and show that dehydroxylation process requires heat.

Keywords: Calcium hydroxide, Non-isothermal kinetics, Thermal dehydroxylation, Thermodynamic parameters

1. Introduction
Calcium hydroxide $Ca(OH)_2$ is an important inorganic compound belonging to the group of hydroxide with brucite structure type. The packing is formed by layers of octahedral Ca sites linked together in (001) plane by strong hydrogen bonds. $Ca(OH)_2$ has been widely used in various technological processes of making new materials or compounds with particular characteristics such as building materials, adsorbents for wastewater including radioactive elements, desulphurizing agents, materials for thermal energy storage and food additives [1-4].
Synthetic $Ca(OH)_2$ compound can be prepared by various methods using different alkaline media and in presence of organic additives or surfactants [5, 6]. However, carbonation by atmospheric CO_2 causes many problems in its use, mainly in the building industry. Several kinetic studies of the carbonation of $Ca(OH)_2$ were performed to examine the possible mechanisms governing this reaction. The carbonation process seems to depend on the particle size and moisture which significantly affects the surface properties of the calcium hydroxide [7, 8].
On the other hand, thermal decomposition of synthetic calcium hydroxide has been subject of several studies because it leads to the formation of calcium oxide CaO nanoparticles more reactive than that derived from the respective limestone, $CaCO_3$ and even from commercial CaO [9, 10]. But some controversial results have been revealed in kinetic studies notably on the estimation of the reaction mechanism and the model which give the best approximation of experimental kinetics. The main divergence is due to experimental conditions, which can be adopted, and to reversible nature of the dehydration produced by the pressure effect of vapor water [11-13]. In the majority of cases, the dehydroxylation process of $Ca(OH)_2$ has been observed under different atmospheres, for temperatures ranging from 300 to 500°C [14, 15]. It is confirmed that dehydroxylation is extremely sensitive to the texture, the form of particles and to the choice of heating rate. The basic mechanism describing the kinetic scheme is often represented by two steps. Thus, Mikhail and Brunner's examination indicate that the dehydroxylation took place at $Ca(OH)_2$/CaO interface through two separate steps [16]. In addition, Brett stated that dehydroxylation started at crystal edges and surface defects followed by the reaction moving inwards into the crystal [17]. According to the nature of decomposition reactions, various mathematical models, listed by Sharp et al [18] were used in order to estimate the kinetic parameters and to simulate the experimental data. Recently, the recommended isoconversional method (Model-Free) proposed by Vyazovkin et al [19, 21] seems the most

adequate for calculating the kinetic parameters (the activation energy, the pre-exponential factor, and the reaction model), because it is applicable to a wide variety of temperature programs and can provide relevant answers to the majority of problems related to the integral methods, as well as the resulting systematic error in activation energy calculations.

In the present work, we have undertaken the preparation of calcium hydroxide $Ca(OH)_2$ by chemical precipitation under reflux method. The thermal kinetics was studied by simultaneous least-square analysis of (TG/DTG and DTA) curves, at different heating rates to reinvestigate the Arrhenius kinetic parameters. The new advanced isoconversional method developed by Vyazovkin [21] was used in order to provide an adequate mechanism of the reaction model which has not yet been well established. The simulation of kinetics for all processes was achieved by Malek's procedure to make sure the correctness of the reaction model [22]. The relationship between kinetic parameters and thermodynamic functions data using isoconversional model is also reported on the basis of thermal analysis techniques.

2. Experimental

2.1. Synthesis

Many different methods have been proposed to synthesize calcium hydroxide $Ca(OH)_2$ [5, 6, 9]. In this study, we have adopted the conventional chemical precipitation process, using calcium chloride $CaCl_2$ and sodium hydroxide NaOH in stoichiometric proportion. Both reagents are supplied by Riedel de Häen and used without any purification. Two initial aqueous solutions of 100 ml containing separate appropriate amounts of $CaCl_2$ and NaOH are prepared respectively, in purified water. The NaOH alkaline solution is added gradually into the $CaCl_2$ solution prior maintained under reflux at 90°C. The mixture was kept at this temperature for 2 hours, then filtered and washed several times with hot water to remove the produced NaCl. Washing is stopped when the test with silver nitrate is negative. The collected material is rinsed with ethanol, dried at 80°C for 2 hours and finally placed in vacuum desiccator.

2.2. Measurements

XRD analyses are performed in order to examine the purity of the sample and to estimate the carbonation process in air. The diagrams were collected using a Siemens D 500 Powder diffractometer equipped with a copper anticathode ($\lambda_{CuK\alpha}$=1.541838 Å) at scanning speed of 0.04°.s^{-1} from 10 to 60°/2θ.

FTIR characterization is used to determine the vibration characteristics of the different bands of $Ca(OH)_2$ and to identify the presence of carbonate species. The experiments were conducted with a Vertex 70 spectrometer provided with a Digitec detector. The KBr pellet method was applied to prepare the samples which were scanned in transmission mode with 4 cm^{-1} resolution, at the range of 4000 to 400 cm^{-1}.

The simultaneous TG/DTG/DTA analyses were carried out on a Labsys^{TM} Evo (1F) Setaram, apparatus, in the non-isothermal conditions from the room temperature up to 800°C, at various heating rate (5, 10, 15 and 20°C/min), in Helium atmosphere with a flow rate of 60 ml.min^{-1}. Small initial mass of samples about 10 ± 2 mg, were placed in an alumina crucible with another empty one used as standard reference. The sample was well dispersed and with negligible depth in order to minimize heat and mass transfer phenomena.

3. Kinetics and thermodynamics studies

According to non-isothermal kinetic theory of heterogeneous solid-gas process, the reaction rate is frequently expressed a function of two variables (the temperature *T* and the extent of conversion *α*) by the well-known equation:

$$\frac{d\alpha}{dt} = k(T).f(\alpha) \qquad \textbf{(1)}$$

Where $\alpha = (W_0-W_t)/(W_0-W_\infty)$, W_t is the mass of the sample at time t, W_0 and W_∞ are the masses of the sample at beginning and end of the mass loss reaction respectively. The dependence of the process rate on temperature is represented by the rate constant, *k(T)*, which is typically parameterized through the Arrhenius equation:

$$k(T) = A\exp\left(-\frac{E}{RT}\right) \qquad \textbf{(2)}$$

Where *A* and *E* are kinetic parameters, the pre-exponential factor and the activation energy, respectively, and R is the universal gas constant.

While, the dependence on the extent of conversion is illustrated by the differential conversion function (reaction model), *f(α)*, which can be related to the experimental data.

For dynamic data obtained at a constant heating rate, $\beta = dT/dt$, this new term and *k(T)* are inserted in Eq. (1) to obtain the Eq. (3):

$$\frac{d\alpha}{dT} = \frac{A}{\beta}\exp\left(-\frac{E}{RT}\right)f(\alpha) \qquad \textbf{(3)}$$

For simple reactions, the evaluation of *f(α)* with an elementary model function is possible. For complex reactions, the functions of *f(α)* are complicated and generally unknown, in this case, the algorithm of simple reaction leads to significant

differences in kinetics data. In order to obtain a reliable kinetic description of the investigated processes, Vyazovkin et al [21] developed an integral kinetic method (advanced isoconversional method), without requiring to specify a model of reaction and proposed the concept of a variable activation energy as a compromise between the actual complexity of solid state reactions and oversimplified methods of describing their kinetics. So, the variation of the activation energy with the extent of conversion is attributed to the relative contribution of each single-step process in the overall reaction rate. This method has advantage to be applied to any reactions of thermal processing and suggests a multiple thermal experiments at different constant heating rates.

3.1. Estimation of the apparent activation energy E_α

The differential isoconversional method suggested by Friedman [23] is based on Eq. (1) in the logarithmic form:

$$\ln\left[\left(\frac{d\alpha}{dt}\right)_{\alpha,i}\right] = \ln\left[A_\alpha f(\alpha)\right] - \frac{E_\alpha}{RT_\alpha} \qquad \textbf{(4)}$$

The apparent activation energy (E_α) is determined from the slope of the plot of $\ln[(d\alpha/dt)_{\alpha,i}]$ versus $1/T\alpha$, at a constant α value. Subscript *i* is the ordinal number of an experiment performed at a given heating rate. Compared to other process for determining the kinetic parameters, the Friedman method is rather accurate because it does not include any forms of mathematical approximations. If the conversion mechanisms are the same at all conversion levels, the isoconversion lines would all have the same slopes.

The advanced isoconversional method proposed by Vyazovkin [21] is an integral nonlinear method that employs a numerical integration computing in small restricted intervals of conversion Δα, by replacing integration over temperature with integration over time. The E_α values can be determined by minimizing the following function:

$$\Phi(E_\alpha) = \sum_{i=1}^{n}\sum_{j\neq i}^{n}\frac{J\left[E_\alpha, T_i(t_\alpha)\right]}{J\left[E_\alpha, T_j(t_\alpha)\right]} \qquad \textbf{(5)}$$

Where the time integral:

$$J\left[E_\alpha, T_i(t_\alpha)\right] = \int_{t_{\alpha-\Delta\alpha}}^{t_\alpha} e^{-E_\alpha/RT_i(t_\alpha)}dt \qquad \textbf{(6)}$$

Here, *T(t)* represents the actual sample temperature, *J* designates the integral with respect to *T(t)* and $T_i(t)$ is the temperature programs.

3.2. Determination of reaction model

The isoconversional method can be applied without knowledge of true *f(α)* function. But this function must be invariant for all heating rates. The invariance can be examined according to procedure proposed by Malek [21, 22]. The Malek's procedure suggests that *f(α)* function is proportional to the *y(α)* and *z(α)* functions that can basically be obtained by a simple transformation of thermogravimetric (TG) data. In non-isothermal conditions, these functions are defined as:

$$y(\alpha) = \left(\frac{d\alpha}{dt}\right)\exp\left(\frac{E}{RT}\right) \qquad \textbf{(7)}$$

$$z(\alpha) = p\left(\frac{E}{RT}\right)\left(\frac{d\alpha}{dt}\right)\frac{T}{\beta} \qquad \textbf{(8)}$$

Where p(*E/RT*) is the expression of the temperature integral. It was suggested that p(*E/RT*) may be accurately estimated by means of the fourth rational expression of Senum and Yang [24]:

$$p(x) = \frac{x^3+18x^2+88x+96}{x^4+20x^3+120x^2+240x+120} \qquad \textbf{(9)}$$

Where *x* is reduced apparent activation energy (*E/RT*). As evident from Eqs. (7) and (8) for calculations of *y(α)* and *z(α)* functions, it is necessary to know the apparent activation energy in non-isothermal conditions. By plotting the *y(α)* and *z(α)* dependence, normalized within the (0, 1) interval, the shape of the function *f(α)* is deduced. Therefore the type of reaction model can be recognized by determining the maxima α_M, α_p and α^∞_p of *y(α), dα/dt and z(α)* functions respectively. The mathematical properties of the *y(α)* and *z(α)* functions for basic kinetic models are summarized in table 1. If there are considerable differences in the shape of the *y(α)* and *z(α)* functions then, we can conclude that the assumption in which the reaction model was considered to be a single-step model has not fulfilled.

3.3. Determination of thermodynamic parameters

From the activated complex theory (transition state) proposed by Eyring et al [26, 27], the relationship linking the pre-exponential factor *A* and the activation entropy *ΔS** may be written by following general equation:

$$A = \left(\frac{e\chi k_B T_P}{h}\right)\exp\left(\frac{\Delta S^*}{R}\right) \qquad \textbf{(10)}$$

Where e = 2.7183 is the Neper number, χ: transition factor, which is unity for monomolecular reactions; k_B: Boltzmann constant; h: Plank constant, and T_p is the average phase transformation temperature peak in four DTA curves (K). The change of the entropy may be calculated according to the formula:

$$\Delta S^* = R \ln\left(\frac{A.h}{e\chi k_B T_P}\right) \quad \textbf{(11)}$$

Since, the thermodynamic functions, enthalpy ΔH^* and Gibbs free energy ΔG^* for the activated complex formation from the reagent were calculated by the following equations:

$$\Delta H^* = E^* - R.T_p \quad \textbf{(12)}$$

$$\Delta G^* = \Delta H^* - T_p.\Delta S^* \quad \textbf{(13)}$$

When E^* is the activation energy obtained from the Friedman method.

Table 1: Schematic diagram of the kinetic model determination [25]

Reaction Model	Symbol	f(α)	y(α)	z(α)
Reaction nth order model (Nucleation/Decay)	Fn/RO	$(1-\alpha)^n$	n<1: Convex n>1: Concave	α_p^∞ depends on exponents
Phase boundary controlled reaction (contracting area, i.e., bidimensional shape or one-half order kinetics)	R2	$2(1-\alpha)^{1/2}$	Convex	0.750
Phase boundary controlled reaction (contracting area ,i.e., tridimensional shape or two-thirds order kinetics)	R3	$3(1-\alpha)^{2/3}$	Convex	0.704
Johnson Mehl Avrami general Equation (Growth of Nuclei)	JMA	$n(1-\alpha)\{-\ln(1-\alpha)\}^{1-1/n}$	n<1: Concave n=1: Linear n>1: $0 < \alpha_m < \alpha_p$	0.632
One dimensional diffusion	D1	$1/2\ \alpha$		
Two dimensional diffusion	D2	$-1/\ln(1-\alpha)$	Concave	0.834
Three dimensional diffusion (Jander's Equation)	D3	$\frac{3(1-\alpha)^{2/3}}{2\{1-(1-\alpha)^{1/3}\}}$	Concave	0.704
Three dimensional diffusion (Ginstling Equation)	D4	$\frac{3}{2[(1-\alpha)^{-1/3}-1]}$	Concave	0.776
Sestak Breggren (Autocatalytic Model)	SB(m,n)	$f(\alpha)=(\alpha)^m(1-\alpha)^n$	$0 < \alpha_m < \alpha_p$	α_p^∞ depends on exponents

4. Results and discussion

4.1. XRD analysis

Figure 1 depicts the XRD patterns of synthesized calcium hydroxide $Ca(OH)_2$, dried at 80°C and the products resulting from calcinations at 400, 600 and 800°C in air for 2 hours. The untreated sample (Figure 1(a)) exhibits a typical diagram of calcium hydroxide (portlandite) which accords with JCPDS (N°.01-073-5492) file. The reflection peaks of $CaCO_3$ are not detected under the observation limitation of XRD. Heating at 400°C (Figure 1(b)), the calcium hydroxide was partially decomposed into CaO by dehydroxylation reaction of OH species. In addition, a small amount of calcite $CaCO_3$ was found in relation to the atmospheric carbonation reaction. When the product is calcined at 600°C (Figure 1(c)), a two phase mixture constituted by calcite and calcium oxide has been observed. Heated at 800°C, the XRD pattern of product shows a single phase attributed to calcium oxide CaO in good agreement with JCPDS (N°.00-02-0968) card. The unit cell parameters of $Ca(OH)_2$ and CaO obtained by least square refinement of the powder XRD data are summarized in table 2.

Table 2: Unit Cell Parameters of $Ca(OH)_2$ and CaO

Samples	a ± 0.0004Å	c ± 0.002Å	S.G	Z
$Ca(OH)_2$	3.5888	4.931	P-3m1	1
CaO	4.8100		Fm3m	4

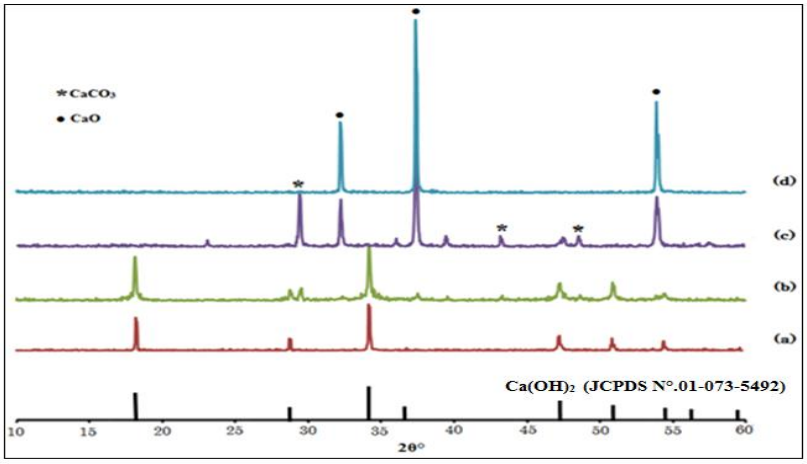

Figure 1: XRD patterns of $Ca(OH)_2$ as prepared and dried at 80°C (a), and its calcined products at 400°C (b), 600°C (c) and 800°C (d)

4.2. FTIR spectroscopy

The FTIR spectrum of $Ca(OH)_2$ as synthesized is shown in figure 2. The narrow absorption band at 3642 cm^{-1} is due to stretching mode of O-H present in the sample. The absorption bands at 1464, 1080 and 873 cm^{-1} are assigned to different vibration modes C-O of carbonate groups CO_3^{2-} [6, 28]. Moreover, there is a tiny dip in the spectra at 2352 cm^{-1} due to the gaseous CO_2. The presence of carbonate groups indicates the slight contamination of sample by atmospheric CO_2 which has not been previously detected by XRD analyses.

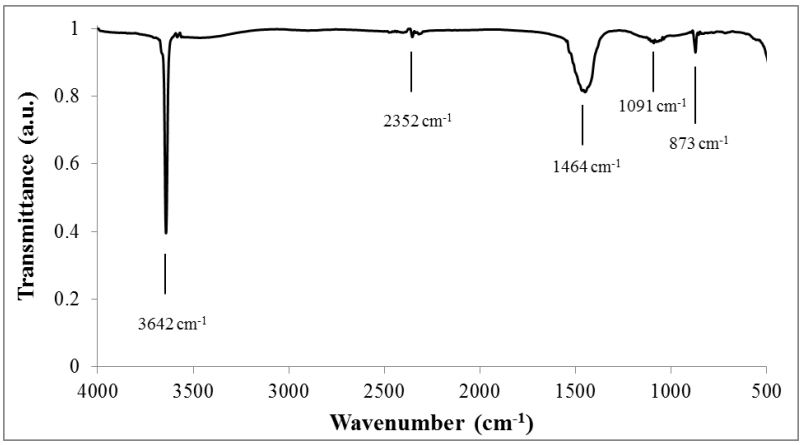

Figure 2: FTIR Spectrum of the $Ca(OH)_2$ dried at 80°C

4.3. Thermal analysis

Thermal measurements of $Ca(OH)_2$ were carried out with non-isothermal conditions. The typical TG, DTG and DTA curves recorded at 10°C.min^{-1} under flowing helium atmosphere are shown in Figure 3. It can be seen from TG curve that thermal dehydroxylation of $Ca(OH)_2$ occurs between temperatures 390 and 476°C, with an endothermic peak at T_{max}=461.6°C corresponding to DTG peak at T_{max}=459.3°C. The mass retained is about 23.5%, very close with the value expected for formation of CaO. At higher temperature (T>600°C), a second mass loss is observed (visible as a weak) due to decarbonation process of sample and corroborates the FTIR results.

4.4. Kinetics study

The kinetic computations on thermal analysis data of $Ca(OH)_2$ have been processed using reliable isoconversional (Model-Free) methods recommended by ICTAC Kinetics Committee, which involve multiple temperatures programs [21]. The experiments were conducted using different constant heating rate β = 5, 10, 15 and 20°C.min^{-1}. Figures 4 and 5 represent the thermal analysis data and the changes of extent of conversion α versus temperature for $Ca(OH)_2$ at four heating rate, respectively.

The TG/DTG curves show an asymmetric character (Figures 4(a) and (b)) and were moves to higher temperatures, with increase in heating rate. From figure 5, it can be seen that all α-T curves at all heating rates have the same shapes (sigmoidal forms), with temperature of the decomposition process between 390 and 500°C. Values of peak temperature (T_p) and the degree of conversion at maximum reaction rate (α_p), at various heating

rates are presented in table 3. Increasing of heating rate leads to increase of the peak temperature value (T_p) from 435.93 to 472.15 °C.

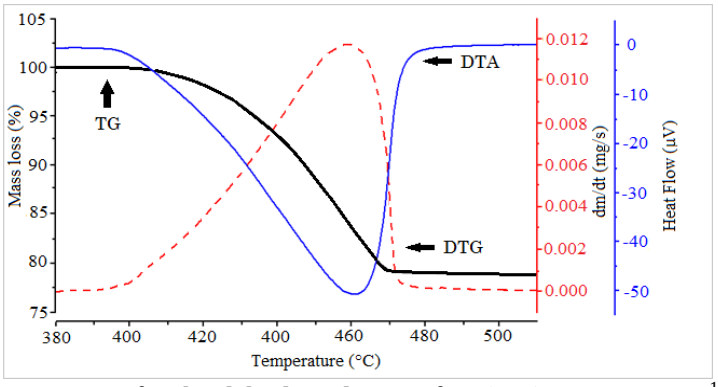

Figure 3: TG/DTG and DTA curves for the dehydroxylation of $Ca(OH)_2$ at 10°C.min^{-1} in He flow

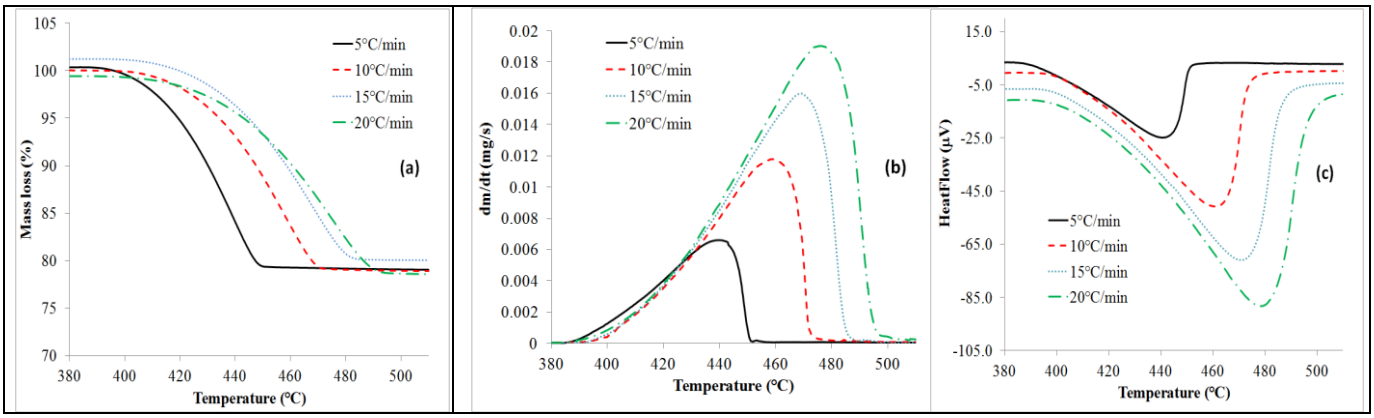

Figure 4: TG/DTG/DTA curves of thermal decomposition of $Ca(OH)_2$ at different heating rates

Table 3: Values of peak temperature (T_p) and extent of conversion at maximum *reaction rate (α_p), for different heating rates*

β(°C.min^{-1})	T_p (°C)	α_p
5	435.93	0.754
10	457.68	0.755
15	471.84	0.763
20	472.15	0.744

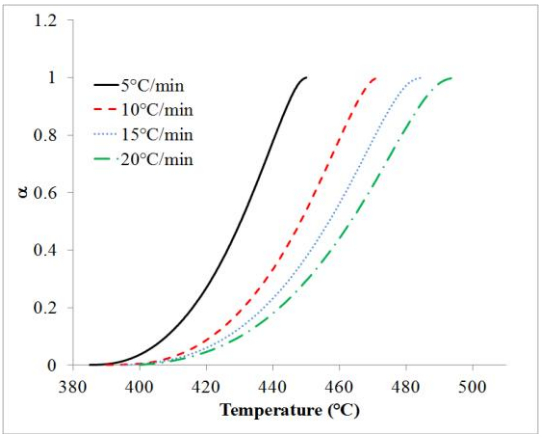

Figure 5: α-T Curves at different heating rates for thermal decomposition of $Ca(OH)_2$

4.4.1. Model-Free estimation of the apparent activation energy Eα

Two representative isoconversional methods were used for determining the apparent activation energy E_α of the dehydroxylation reaction of $Ca(OH)_2$, the differential method of Friedman and advanced isoconversional

(integral) method of Vyazovkin. Figure 6 shows the dependence of the activation energy E and the apparent isoconversional (Friedman) intercepts (Eq. 4) versus the extent of conversion α, in the range [0.1-0.9].

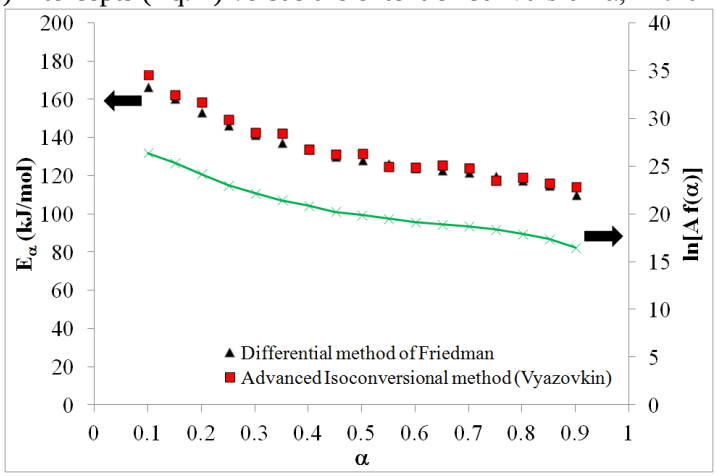

Figure 6: Variation of activation energy *Eα* with extent conversion α

The Friedman and Vyazovkin methods exhibit similar behavior of activation energy E_α which is represented by a decreasing function of conversion α. The concordance between both methods was also mentioned by several authors [29, 30]. According to Opfermann [31] and Zelic [32], which have used the isoconversional integral method of Flynn, Wall and Ozawa (FWO) to their experimental data, the variation of the activation energy indicates that the overall dehydroxylation process is likely performed at least by two elementary reaction steps. The first step occurs rapidly at the beginning and corresponds to the kinetic scheme of an endothermic reversible reaction. The second step which characterizes the main reaction is represented by an irreversible reaction with lower activation energy. According to the reaction mechanism proposed by Mattsuda et al [33], the dehydroxylation process scheme could be written as:

$$Ca(OH)_2 \underset{\text{Fast}}{\overset{\text{Step 1}}{\rightleftharpoons}} \text{"CaO, } H_2O\text{"} \xrightarrow[\text{Low}]{\text{Step 2}} CaO$$

In the following, the study will take counted only of the second step recognized as determinative because the first restricted step is so fast that is not obvious. In this case, the activation energy is considered practically invariable in the conversion range [0.2-0.8] with the average values *E* of 130.67 kJ.mol^{-1} and 132.20 kJ.mol^{-1} for Friedman and Vyazovkin methods respectively.

4.4.2. Determination of kinetic model

The kinetic model that can be used to describe the experimental data was determined by the isoconversional Malek procedure. The variation of *y(α)* and *z(α)* functions with conversion α, calculated using Eqs. (7) and (8) respectively and normalized within (0, 1) are indicated in Figures 7 and 8. The shapes of the *y(α)* and *z(α)* plots are practically unchanged with respect to heating rate *β*. For calculations of the above functions, the apparent activation energy value of *E* = 132.20 kJ.mol^{-1} evaluated from Vyazovkin's method was used.

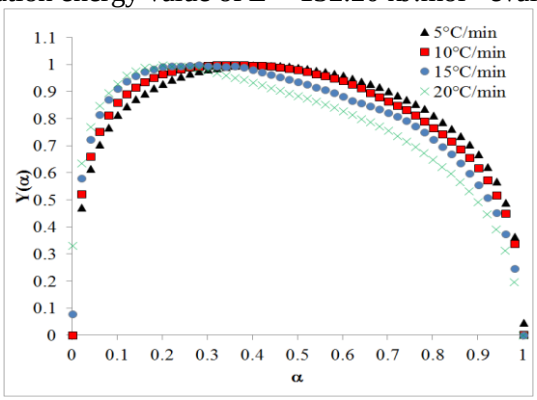

Figure 7: *The plots of y(α) functions versus α at different heating rates*

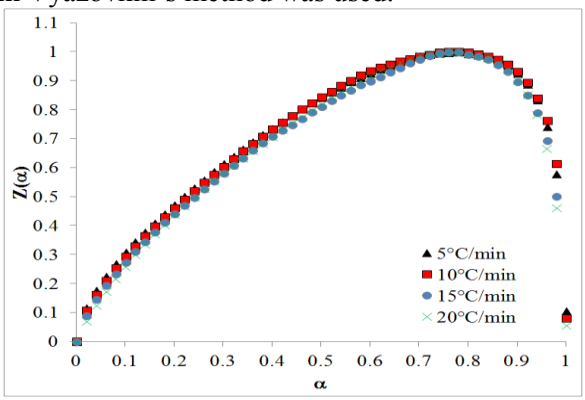

Figure 8: *The plots of z(α) functions versus α at different heating rates*

As was noticed, the data in table 4 which has been extracted from figures7 and 8, show that α_M and α^{∞}_p values depend on the heating rate. The maxima of *y(α)* functions are observed in the range of 0.203 to 0.439, whereas the maxima of *z(α)* functions has a values from 0.767 to 0.777. Thus knowing that $0< \alpha_M <0.754$ and $\alpha^{\infty}_p = 0.770$, the autocatalytic SB (Sestak-Berggren) model [34, 35] in which $f(\alpha) = \alpha^m.(1-\alpha)^n$ (where *m* and *n* represent the kinetic exponents) seems to be the most suitable for the dehydroxylation process of calcium hydroxide. By applying the SB model, the simulation of TG experiments using non-linear regression method gives the kinetic parameters values illustrated in table 5 and the kinetic triplet is established as follow:

$Ln\ A = 16.85\ min^{-1}$ $E = 132.20\ kJ.mol^{-1}$ $f(\alpha) = \alpha^{0.203}.(1-\alpha)^{0.380}$

Table 4: Values of α_M , α_p and α_p^{∞} at different heating rates

β(°C.min^{-1})	α_M	α_p	α_p^{∞}
5	0.439	0.754	0.777
10	0.346	0.755	0.769
15	0.278	0.763	0.767
20	0.203	0.744	0.769
Average	**0.316**	**0.754**	**0.770**

Table 5: Kinetic Parameters of thermal dehydroxylation of $Ca(OH)_2$

β(°C.min^{-1})	**A(min^{-1})**	**Ln A**	**m**	**n**
5	$2.16.10^7$	16.8881	0.2623	0.3487
10	$2.16.10^7$	16.8899	0.2976	0.3810
15	$2.00.10^7$	16.8103	0.1474	0.3835
20	$1.97.10^7$	16.7965	0.1036	0.4072
Average	**$2.07.\ 10^7$**	**16.8460**	**0.203**	**0.380**

For autocatalytic model, the average pre-exponential factor was found to be $A = 2.07\ 10^7\ min^{-1}$ (Ln A = 16.85). The obtained value of Ln A is consistent with average value of Friedman isoconversional intercept (Ln[Af(α)] = 16.23, Figure 6).

By introducing the kinetic parameters values into Eq. (1), Eq. (14) can be obtained:

$$\frac{d\alpha}{dt} = 2.07\,10^7 \exp\left(\frac{-132.20}{RT}\right) \alpha^{0.203}(1-\alpha)^{0.380} \qquad \textbf{(14)}$$

From Eq. (14), the plots of *α* and *dα/dt* against temperature at different heating rates are reconstructed in Figures 9 and 10 respectively. It can be seen that the reconstructed curves are in good agreement with experimental curves, thus confirming the validity of obtained results.

The first step that is not included in our calculations did not cause deviation on the simulated curves; this means that the overall process is practically dominated by the irreversible reaction (second step). According to Opfermann [31], the first step is practically negligible because it amounts to only 3,3% of the total mass loss.

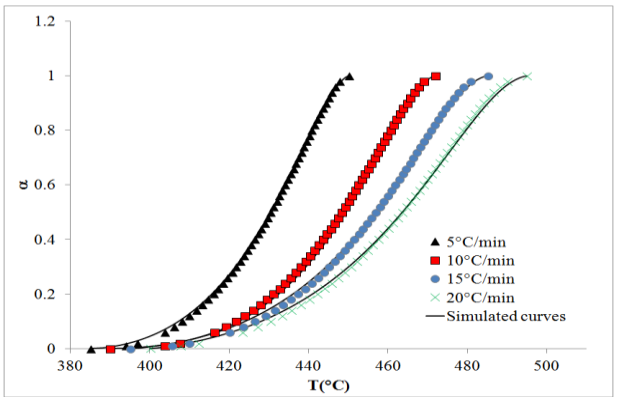

Figure 9: Comparison between the experimental and reconstructed (α-T) curves of non-isothermal experiments at different heating rates

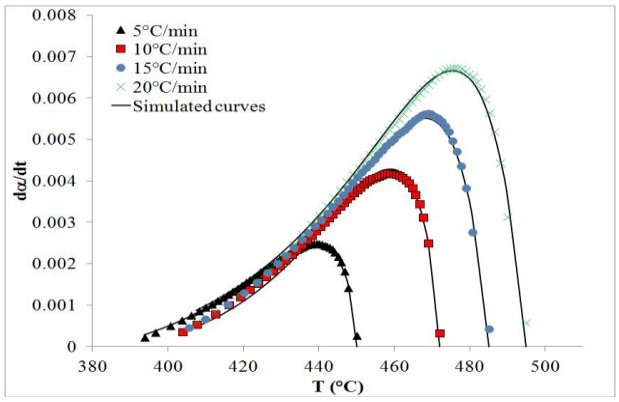

Figure 10: Comparison between the experimental and reconstructed (dα/dt) curves of non-isothermal experiments at different heating rates

4.5. Determination of thermodynamic parameters

On the basis of isoconversional method, the thermodynamic parameters (*ΔS*, ΔH*, ΔG**) for the formation of activated complex were calculated from Eqs.(10)-(13) and presented in table 6. The negative values of *ΔS** for all heating rates showed that the formation of the activated complex from the initial state is connected with a decreasing of entropy, i.e. the activated complex is "more organized" structure and the formation process may be classify as "slow" [36]. The values of *ΔH** were found to be in agreement with the average value of the activation energy obtained by the method of Friedman (E = 130.67 kJ.mol^{-1}). The positive values of *ΔH** and *ΔG** confirm the endothermic effects previously observed in DTA curves and indicated that the dehydroxylation of $Ca(OH)_2$ is a non- spontaneous process at room temperature.

Table 6: Themodynamic parameters of $Ca(OH)_2$

β(°C.min^{-1})	ΔS* (J/K.mol)	ΔH* (kJ/mol)	ΔG* (kJ/mol)
5	-120.00	124.34	209.44
10	-120.26	124.16	212.05
15	-121.08	124.04	214.25
20	-121.20	124.04	214.37
Average	**-120.64**	**124.14**	**212.53**

Conclusion

The kinetics of the non-isothermal dehydroxylation of calcium hydroxide was accurately determined from a series of thermo-analytical experiments at different constant heating rates. The apparent activation energy (E) was calculated by differential (Friedman) and advanced (Vyazovkin) isoconversional methods (Model-Free) without previous knowledge regarding the conversion model fulfilled by the reaction. From the two methods, the calculated activation energies lead to similar behaviors represented by decreasing functions versus α. Eα assumes a high value at the beginning of the dehydroxylation reaction and drops when increasing α, to average values of 130.67 kJ.mol^{-1} and 132.20 kj.mol^{-1} for Friedman and Vyazovkin methods respectively. This dependence of the activation energy is an indication that the overall reaction involves two steps, corresponding to a main reaction with a low activation energy value, preceded by another reaction with higher activation energy.

By applying the Malek's procedure, the appropriate reaction model characterizing the process studied was established. The shapes of *y(α)* and *z(α)* indicate that the autocatalytic SB model is the most probable kinetic model for describing the dehydroxylation process of calcium hydroxide. From SB model, the simulation of TG experiments which leads to the best fit, using the non-linear regression leads to the following kinetic parameters values:

$$\boldsymbol{LnA = 16.85,\ E = 132.20\ kJ.mol^{-1}\ and\ f(\alpha) = \alpha^{0.203}.(1-\alpha)^{0.380}}$$

And the kinetic equation as:

$$\frac{d\alpha}{dt} = 2.07\,10^{7}\exp\left(\frac{-132.20}{RT}\right)\alpha^{0.203}(1-\alpha)^{0.380}$$

The thermodynamic parameters (*ΔS**, *ΔH**, *ΔG**) of the dehydroxylation of $Ca(OH)_2$ are obtained and indicate that the reaction is directly related to the introduction of heat and is non-spontaneous process.

Acknowledgment-The authors are grateful for the financial support of this project by research Grant (SCH04/09) of University of Mohammed V-Agdal, Morocco**.**

References

1. Arliguie G., Grandet J., Ollivier J. P., *Mater. Struct.*, 18 (1985) 263.
2. Zhang F., Parker J. C., Brooks S. C., Watson D. B., Jardine P. M., Gu B., *J. Hazard. Mater.*, 178 (2010) 42.
3. Bin Z., Chunmei L., Lixia J., *Proc.CSEE*, 29 (2009) 32.
4. Murthy M. S., Raghavendrachar P., Sriram S. V., *Sol. Energy*, 36 (1986) 53.
5. Daniele V., Taglieri G., *J. Cult. Herit*., 13 (2012) 40.
6. Liu T., Zhu Y., Zhang X., Zhang To., Zhang Ta., *Mater. Lett*., 64 (2010) 2575.
7. Otsu A., Tsuru K., Maruta M., Munar M. L., Matsuya S., Ishikawa K., *Dent. Mater.*, 31 (2012) 593.
8. Van Balen K., *Cem. Concr. Res*., 35 (2005) 647.
9. Mirghiasi Z., Bakhtiari F., Darezereshki E., Esmaeilzadeh E., *J. Ind. Eng. Chem.*, 20 (2014) 113.
10. R Bruce K., Gullet B. K. , Beach L. O., *AIChE J.*, 35(1989) 37.

11. Galwey A. K., Laverty G. M., *Thermochim. Acta*, 228 (1993) 359.
12. Chen D., Gao X., Dollimore D., *Thermochim. Acta*, 215(1993) 65.
13. Irabien A., Viguri J. R., Ortiz I., *Ind. Eng. Chem. Res.*, 29 (1990) 1599.
14. Schaube F., Koch L., Wörner A., Müller-Steinhagen H., *Thermochimi. Acta*, 538 (2012) 9.
15. Dutta S., Shirai T., *Chem. Eng. Sci.*, 29 (1974) 2000.
16. Mikhail R. S., Brunnauer S., Copeland L. E., *J. Colloid Interface Sci*.,21 (1966) 395.
17. Brett N. H., *Miner. Mag.*, 37 (1969) 244.
18. Sharp J. H., Brindley G. W., Narahari Achar B. N., *J. Am. Ceram. Soc*., 49 (1966) 379.
19. Vyazovkin S., in Recent advances, Techniques and Applications, Elsevier, 2008.
20. Vyazovkin S., *J. Comput. Chem.*, 23 (2001) 178.
21. Vyazovkin S., Burnham A. K., Criado J. M., Pérez-Maqueda L. A., Popescu C., Sbirrazzuoli N., *Thermochim. Acta*, 520 (2011) 1.
22. Malek J., *Thermochim. Acta*., 200 (1992) 257.
23. Friedman H. L., *J. Polym. Sci. Part C: Polym. Symp*., 6 (1964) 183.
24. Senum G. I., Yang R. T., *J. Therm. Anal*., 11 (1977) 445.
25. Jankovic B., Mentus S., Jankovic M., *J. Phys. Chem. Solids*, 69 (2008) 1923.
26. Boonchom B., *J. Therm. Anal. Calorim.*, 98 (2009) 863.
27. Vlaev L., Georgieva V., Genieva S., *J.Therm. Anal. Calorim.*, 88 (2007) 805.
28. Blesa M. J., Miranda J. L., Moliner R., *Vib. Spectrosc*., 33 (2003) 31.
29. Sbirrazzuoli N., *Macromol. Chem. Phys.*, 208 (2007) 1592.
30. Budrugeac P., *J. Therm. Anal. Calorim.*, 68 (2002) 131.
31. Opfermann J., *J. Therm. Anal. Calorim.*, 60 (2000) 641.
32. Zelic J., Ugrina L., Jozic, The First International Proficiency Testing Conference, Sinaia, 2007.
33. Matsuda H., Ishizu T., Lee S. K., Hasatani M., *Kagaku Kogaku Ronbun*, 11 (1985) 542.
34. Simon P., *Thermochim. Acta*, 520 (2011) 156.
35. Sestak J., Berggren C., *Thermochim. Acta*, 3 (1971) 1.
36. Vlaev L., Nedelchev N., Gyurova K., Zagorcheva M., *J. Anal. Appl. Pyrolysis*, 81 (2008) 253.